Imaging metabolic syndrome

*Weiping Han, Kai-Hsiang Chuang, Young-Tae Chang, Malini Olivo, S. Sendhil Velan, Kishore Bhakoo, David Townsend, George K. Radda**

Metabolic syndrome is a fast growing public health burden for almost all the developed countries and many developing nations. Despite intense efforts from both biomedical and clinical scientists, many fundamental questions regarding its aetiology and development remain unclear, partly due to the lack of suitable imaging technologies to visualize lipid composition and distribution, insulin secretion, β-cell mass and functions *in vivo*. Such technologies would not only impact on our understanding of the complexity of metabolic disorders such as obesity and diabetes, but also aid in their diagnosis, drug development and assessment of treatment efficacy. In this article we discuss and propose several strategies for visualization of physiological and pathological changes that affect pancreas and adipose tissue as a result of the development of metabolic diseases.

Molecular imaging

For centuries, physicians have been striving to observe the structures and functions of the human body without the need to cut it open or to perform a biopsy. The discovery of X-rays in 1895 laid the foundation for the major advances made much later in the 1970s, *i.e.* taking a picture of the human body by X-ray to give a detailed image. At the same time, magnetic resonance imaging (MRI, see Box 1) was discovered and developed for medical imaging, as was the use of radioisotopes and ultrasound. A modern radiology department uses all these techniques for the diagnosis and therapy evaluation of a range of diseases.

In parallel, life scientists wanted to look inside the living cells to see the architecture and makeup of life at the molecular level. The microscope in the first instance, followed by the use of light, electrons, X-rays and magnetic signals to observe molecular details of structure and function in isolated cells have all contributed to the enormous advances that have been made in understanding life. Several imaging tools, their resolution and applications in the biomedical sciences are depicted in Fig 1. In this genomic era, imaging the working products of the genome inside a living cell, in

a model organism of human disease (*e.g.* mouse models) and in human patients is one of the most powerful approaches to advance our knowledge. In the field of molecular medicine, imaging is also a way to link pre-clinical biomedical research and clinical practice. Imaging biomarkers can provide surrogate endpoints for clinical trials or shortcuts to drug development.

By definition, molecular imaging is the non-invasive visualization in space and time of normal as well as abnormal cellular processes at a molecular or genetic level. It can be used to characterize and measure particular biological processes in living organisms. The term 'molecular imaging' is used in a variety of ways to describe (1) the imaging of endogenous molecules that are present in a living system; (2) the use of foreign targeted or activatable reporter agents that sense specific molecular targets or cellular processes; (3) the use of labelled or natural substrates to follow particular pathways and (4) the introduction of genes to express protein products that can be detected directly or indirectly.

In this article, rather than an extensive review of the literature, we present our own perspective of how an important clinical problem—the metabolic syndrome—can be tackled using molecular imaging tools. Our group includes a highly multi-disciplinary team of engineers, physicists, chemists, biologists

Singapore Bioimaging Consortium, Agency for Science Technology and Research (A*STAR), Singapore, Singapore.

Corresponding author: Tel: +65-6478-8721; Fax: +65-6478-9957; E-mail: george.radda@sbic.a-star.edu.sg

and medical researchers, working together as a team to bring individual ideas and technical knowledge. The problem we chose to address, metabolic syndrome, describes a group of metabolic abnormalities that raise the risk of cardiovascular disease and type 2 diabetes, including hyperinsulinaemia, dyslipidaemia, central obesity and hypertension (Reaven, 1993). Here we will consider obesity and type 2 diabetes in particular and will use these diseases as examples to illustrate how some of the outstanding questions in the area may be approached by using novel imaging techniques. We will discuss the limitations of existing technologies and examine some recent developments that might provide alternative ways of thinking in the field. It will become clear that such solutions require close collaboration between scientists in the engineering and physical sciences with biomedical and clinician scientists.

Imaging ectopic fat accumulation

Ectopic lipid deposition, *i.e.* lipid accumulation in tissues/organs other than white adipose tissue (WAT), such as liver and muscle, is often associated with metabolic abnormalities, including insulin and leptin resistance (Muoio & Newgard, 2006). One of the questions in the metabolic disease field is how lipids are accumulated ectopically, and which particular lipid species cause the most severe damage leading to insulin and leptin resistance during diabetes and obesity development.

Arguably, magnetic resonance is probably the most suitable technology to study the role of lipids non-invasively *in vivo* (see Box 2). Although measurement of total fat and three-dimensional (3D) reconstruction and quantification of various fat depots can be done routinely and reliably with MRI aided with

Glossary

Arterial spin labelling
A functional magnetic resonance imaging method used in measuring blood flow.

β-cell
A type of endocrine cell in the pancreas that secretes insulin.

Cardiovascular disease
A class of diseases that involve the heart or blood vessels, *e.g.* stroke.

Contrast agents
A substance used to enhance the contrast of structures or fluids within the body in medical imaging.

Dynamic nuclear polarization (DNP)
Results from transferring spin polarization from electrons to nuclei, thereby aligning the nuclear spins to the extent that electrons are aligned. DNP is one of several techniques for hyperpolarization.

Dyslipidaemia
A condition with abnormal amount of lipids in the blood. Hyperlipidaemia, a form of dyslipidaemia, is often seen in people with hyperinsulinaemia.

Exocytosis
A process by which a cell directs the contents of secretory vesicles out of the cell membrane.

Gradient spin echo
A variety of MRI sequences that allow the measurement of diffusion coefficients.

Hyperinsulinaemia
A condition in which there are excess levels of circulating insulin in the blood. It is often found in people with type 2 diabetes.

Hypertension
A chronic medical condition in which the blood pressure is elevated. Persistent hypertension increases the risk for strokes, heart attacks and heart failure.

Insulin
A hormone released from pancreatic β-cells, which is central to regulating energy and glucose metabolism in the body.

Isotopomer analysis
It provides the possibility of distinguishing between molecules of the same compound on which only one atom contains an isotope and those with two or more atoms labelled by the same isotope; it allows the measurement of isotope isomer distributions to calculate the fluxes through a biochemical network.

Krebs cycle
A series of enzyme-catalysed chemical reactions of central importance in all living cells that use oxygen for cellular respiration.

Leptin
A hormone released from white adipose tissue, which is a key regulator of energy homeostasis. Defective leptin signalling is the leading biological basis for obesity.

Magnetic resonance spectroscopy
A specialized technique that allows detection of biochemical reactions non-invasively *in vivo*, *e.g.* measurement of ATP and phosphocreatine levels in phosphorus spectroscopy.

Obesity
A medical condition with excess body fat accumulation. Body mass index is used to define people as overweight (BMI between 25 and 30 kg/m^2) or obese (BMI $\geq$ 30 kg/m^2).

Pancreatic islets
The pancreatic islets contain the endocrine cells in the pancreas, including glucagon-secreting α-cells and insulin-secreting β-cells.

PET (positron emission tomography)
A nuclear medicine imaging technique which produces a 3D image or picture of functional processes in the body.

Radioisotope
An atom with an unstable nucleus, characterized by excess energy that may be imparted to a newly created radiation particle within the nucleus, or to an atomic electron.

Type 2 diabetes
A disorder that is characterized by high blood glucose in the context of relative insulin deficiency and insulin resistance. About 6% of the world population suffers from type 2 diabetes.

Ultrasound
Cyclic sound pressure with a frequency greater than the upper limit of human hearing, which is approximately 20,000 Hz.

X-ray
A form of electromagnetic radiation, with wavelength in the range of 0.01–10 nm, corresponding to frequencies in the range of 3×10^{16}–3×10^{19} Hz.

BOX 1: Magnetic resonance imaging and magnetic resonance spectroscopy

MRI/MRS is based on a physical phenomenon called nuclear magnetic resonance (NMR). A positively charged hydrogen nucleus (proton) exposed to a magnetic field can absorb energy from the magnetic pulse and radiate this energy out at a particular frequency (the resonance frequency (RF), $\sim$64 MHz at 1.5 T). As the perturbed proton returns to its equilibrium state (relaxation), the RF wave can be detected by a radiofrequency coil and the relaxation process can be described by two-time constants—longitudinal relaxation time (T_1) and transverse relaxation time (T_2). T_1 and T_2 reflect the micro- or macro-environment of the proton such as diffusion, magnetic susceptibility, temperature, binding to proteins and flow. Therefore, pathologies that change these properties, *e.g.* haemorrhages, can be detected. The resonance frequencies of protons in different chemicals are characteristically 'shifted' by the chemical environments of the protons and therefore spectral analysis of the NMR signal enables identification and quantification of metabolites in tissues and *in vivo*. Besides ^{1}H, nuclei of atoms, including ^{13}C, ^{23}Na and ^{31}P, also have magnetic properties. They can be used to study a range of chemicals in living systems that contain these atoms.

1D MRS (magnetic resonance spectroscopy) (Liu et al, 2010; Springer et al, 2010), it remains a challenge to determine the extent of saturated and unsaturated lipids within a tissue compartment. In particular, detecting the saturated and unsaturated lipids of intramyocellular lipid (IMCL) and extra- myocellular lipid (EMCL) pools in skeletal muscle is a challenge because of the small spectral chemical shift between the olefinic protons of the two lipid pools (Fig 2A). The degree of unsaturation within the IMCL and EMCL pools is of significant clinical importance (Boesch, 2007), as the effects of fatty acid on
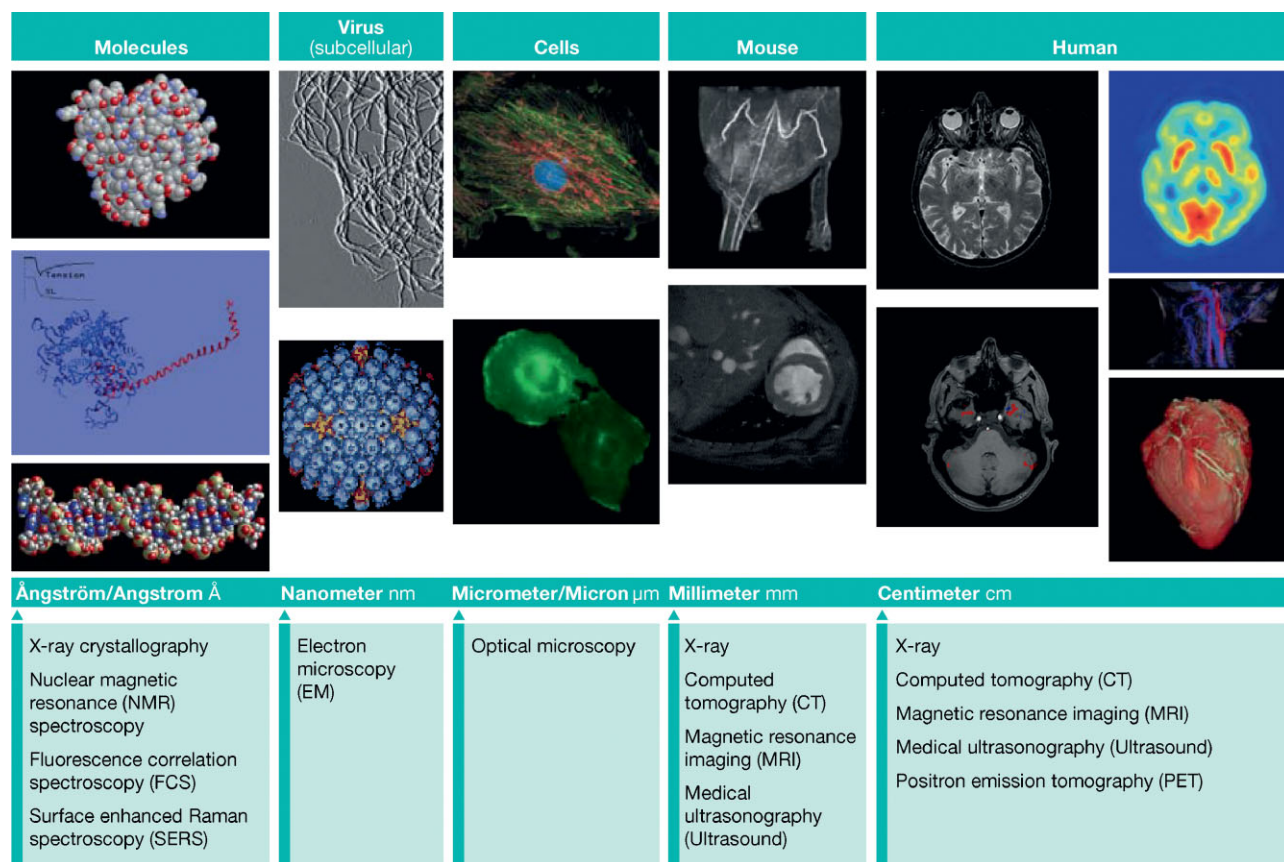

Figure 1. **Imaging modalities, their spatial resolution and applications.** Bioimaging encompasses a range of imaging modalities that provide spatial and functional analyses from molecules in the angstrom level to human brain and heart in the centimetre level. NMR, nuclear magnetic resonance; SERS, surface-enhanced Raman scattering; CT, computed tomography; MRI, magnetic resonance imaging; PET, positron emission tomography.

<div style="border:1px solid #1a6ca8; padding:1em;">

BOX 2: The advantages of magnetic resonance to study the role of lipids non-invasively *in vivo*

MR is well suited for studying lipids non-invasively in humans or animal models of diabetes or obesity. First, the signals from fat and water in tissue are relatively easy to separate in MR images, and it is routine to use MRI in clinical studies to evaluate fat distribution. Second, ^{1}H magnetic resonance spectroscopy (MRS) can be used to measure the amount of 'liquid lipid' in triglycerides, *i.e.* lipids that have fast movement and not lipids that compose structures like membranes. Third, signals in the MR spectra from saturated and unsaturated fatty acid chains can be distinguished, providing a route for the molecular characterization of

in vivo fat. Fourth, intracellular and extracellular lipid signals in skeletal muscle and possibly in other organs can be separated by ^{1}H MRS (Boesch et al, 1997). All these approaches have been used in humans and rodent models for obesity and diabetes, and thus provide a powerful link between pre-clinical investigations of animal models and clinical studies of patients. For example, the signal from IMCL correlates with insulin resistance in both human (Meex et al, 2010) and animal models such as the Zucker rat (Korach-Andre et al, 2005).

</div>

metabolic signalling and energy metabolism are modulated by degree of unsaturation (Vessby et al, 2002). To overcome the limitations of inadequate spectral dispersion in 1D MRS measurements, one possible solution is to use spatially resolved 2D MRS techniques (Fig 2B). A recent study demonstrated the

2D approach to estimate the degree of unsaturation within IMCL pool, and found a direct link between the extent of obesity and unsaturated IMCL, lending further support to the current knowledge of dysregulated lipid metabolism in obesity (Velan et al, 2008).
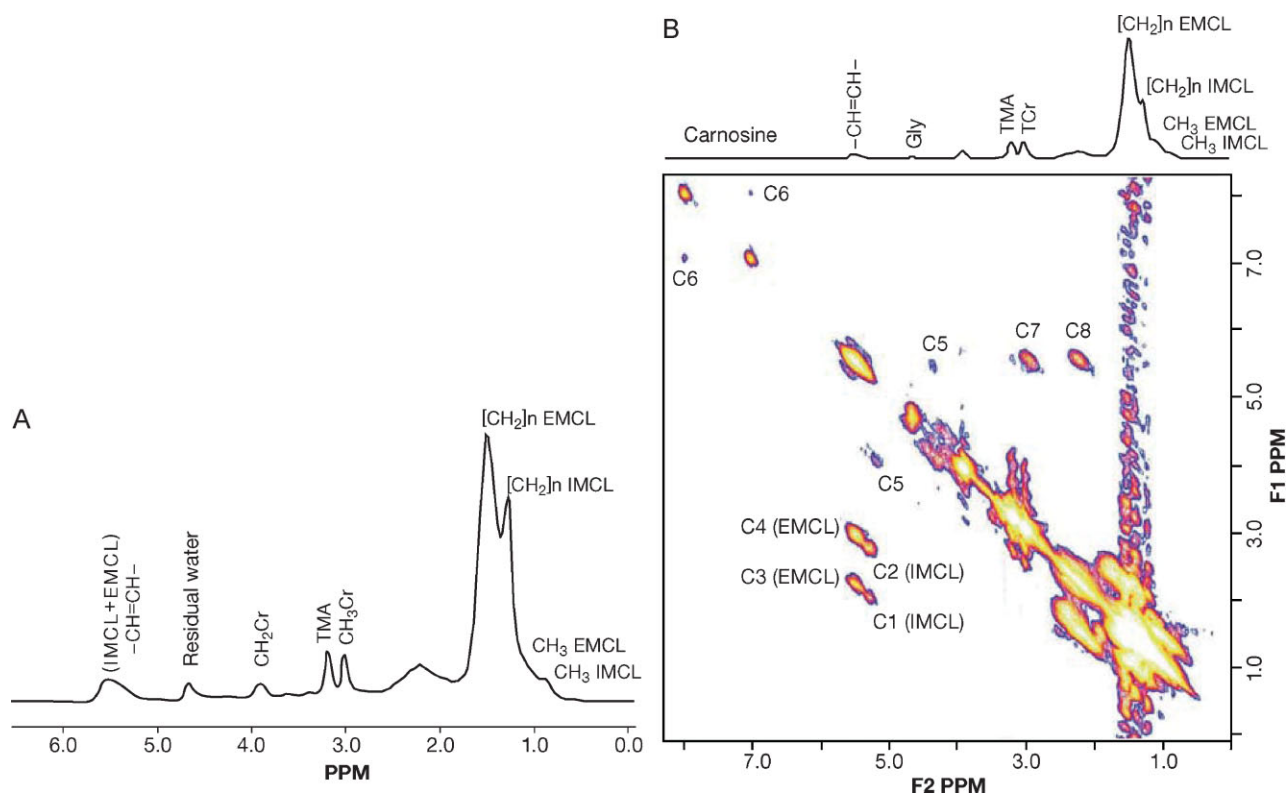

Figure 2. Localized 1D and 2D MRS of skeletal muscle.

A. 1D spectrum including the olefinic protons (–CH=CH–) obtained by 1D point-resolved spectroscopy (PRESS) from soleus muscle. The CH_3 and $(CH_2)_n$ from the IMCL and EMCL pools are seen, along with creatine and trimethyl amine (TMA) protons.

B. Localized 2D correlation spectrum (L-COSY) recorded from soleus muscle of a normal weight healthy subject. The spectrum shows the diagonal and cross-peaks from various resonances of both IMCL and EMCL pools. The cross-peaks due to olefinic (–CH=CH–) and allylic methylene protons ($CH_2CH=CH$) and diallylic methylene protons (–CH=CH–CH_2–CH=CH–) permits estimation of degree of unsaturation.

Imaging of insulin secretion and insulin granule exocytosis in model organisms

Understanding insulin secretion and its regulation mechanisms *in vivo* as well as being able to measure β-cell mass over the disease progression is instrumental for drug target screening, validation and for evaluation of therapeutic strategies. Since the discovery of insulin almost a century ago, research efforts have been focussed on understanding insulin secretion mechanisms, and more recently, on the molecular regulation of insulin granule exocytosis. These studies established cellular mechanisms governing insulin secretion (Fig 3), but many of its details have not been tested in *in vivo* settings, due to the lack of suitable tools to measure and quantify insulin secretion at high spatial and temporal resolutions.

Traditionally, insulin secretion is measured by enzyme-linked immunosorbent assay (ELISA) or radioimmunoassay (RIA). These methods suffer from poor temporal resolution, complete lack of spatial resolution and delayed results. In model organisms, optical imaging of genetically introduced exocytosis markers may provide an alternative, with high spatial and
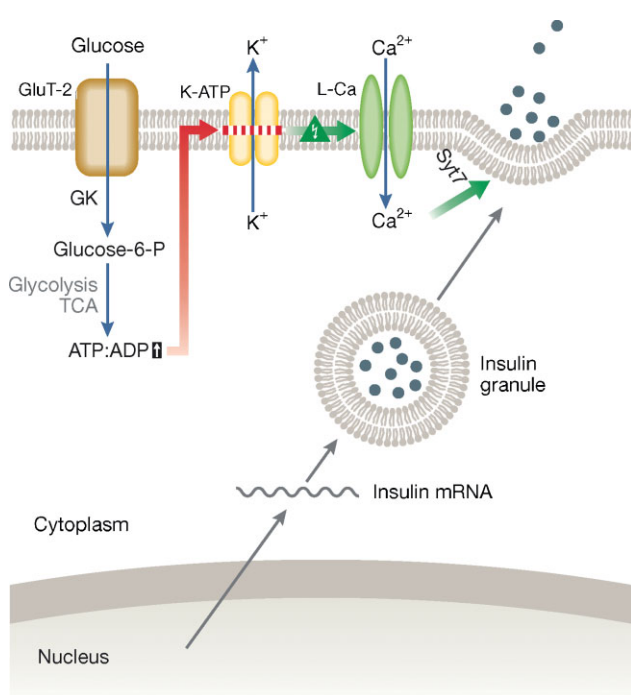

Figure 3. Cellular and molecular regulation of insulin secretion. The cellular events leading to insulin secretion start with a rise in glucose level in the blood, which quickly leads to glucose uptake into pancreatic β-cells. Glucose in the cells then undergoes glycolysis and Krebs cycle to produce ATP, resulting in an increased ATP/ADP ratio, and consequent closure of K_{ATP}-channels. Membrane depolarization from K_{ATP}-channel closure opens L-type calcium channels, allowing calcium influx into the cells, which then triggers insulin granule exocytosis and the release of insulin into blood. GluT-2, glucose transporter 2; GK, glucokinase; TCA, tricarboxylic acid cycle; Syt7, synaptotagmin-7; K-ATP, ATP-sensitive potassium channel; L-Ca, L-type calcium channel.

temporal resolutions, along with instantaneous quantitative information. Figure 4 depicts one strategy for visually monitoring insulin granule movement and exocytosis, and for providing instantaneous quantification of insulin secretion. The optical sensor for exocytosis can be genetically introduced into mouse β-cells under the control of mouse insulin I promoter (Lu et al, 2009) or other β-cell specific promoters. Intravital fluorescent microscopic imaging may be used to examine insulin granule exocytosis systemically by tail vein injections of reagents that impact insulin secretion. Such a strategy may also be combined with surface-enhanced Raman spectroscopic (SERS) detection of insulin and glucose as detailed in Fig 5. In this SERS-based approach, a SERS tag (*e.g.* an organic molecule immobilized on a gold nanoparticle) serves to label and track an analyte such as insulin. Although label-free detection of analytes on a nanoparticle surface is theoretically possible, this has not been demonstrated in a published study. Since SERS tags use molecules tethered to the surface of gold or silver nanoparticles, it has limited or no toxicity (Faulds et al, 2004), particularly in gold-based systems. In some cases, the whole SERS active substrate could be implanted in mouse to obtain quantitative sensing of glucose (Stuart et al, 2006) upon laser excitation (see Fig 5B for an example of an implantable substrate prepared by lithographic techniques). Moreover, advantages such as high information content, multiplexing capability, lack of extensive sample preparation, high tissue penetration and a highly sensitive detection limit to the level of single molecules (Qian et al, 2008) have led to various applications of SERS in biosensing, *e.g.* in cells (Kim et al, 2006), tissues (Zhang et al, 2008) and circulating tumour cell detection in human whole blood (Hu et al, 2007). The essential requirement for the SERS-based method is that an analyte or its reporter lies close to the nanoparticles or nano-roughened surface of noble metals such as gold or silver. Table 1 lists the means to attach an analyte molecule to the metal surface and its applications. The SERS technique has been used in mouse models for *in vivo* tumour targeting and detection (Keren et al, 2008; Qian et al, 2008; von Maltzahn et al, 2009; Xiao et al, 2009; Zavaleta et al, 2009). In the context of metabolic sensing, the promise of SERS lies on the detection of glucose and its derivatives, and of insulin and other peptide hormones using SERS-active nanoparticles attached to a fibre-optic sensor (Zhang et al, 2007). Even though optical fibre-based SERS biosensing is still at its infancy (Shi et al, 2009), we anticipate that this technique will be of great use as the fibre can be readily configured for *in vivo* applications to allow SERS-based metabolic studies in living animals in the near future.

In vivo imaging of pancreatic β-cell mass and function

Besides defective insulin secretory processes, reduced β-cell mass with consequent decreased production and secretion of insulin also contributes to the development of type 2 diabetes. Whether there is a minimal number of pancreatic islets needed to maintain proper blood glucose levels or a sizeable reduction (*e.g.* by 50%) in β-cell mass directly results in diabetes is not yet
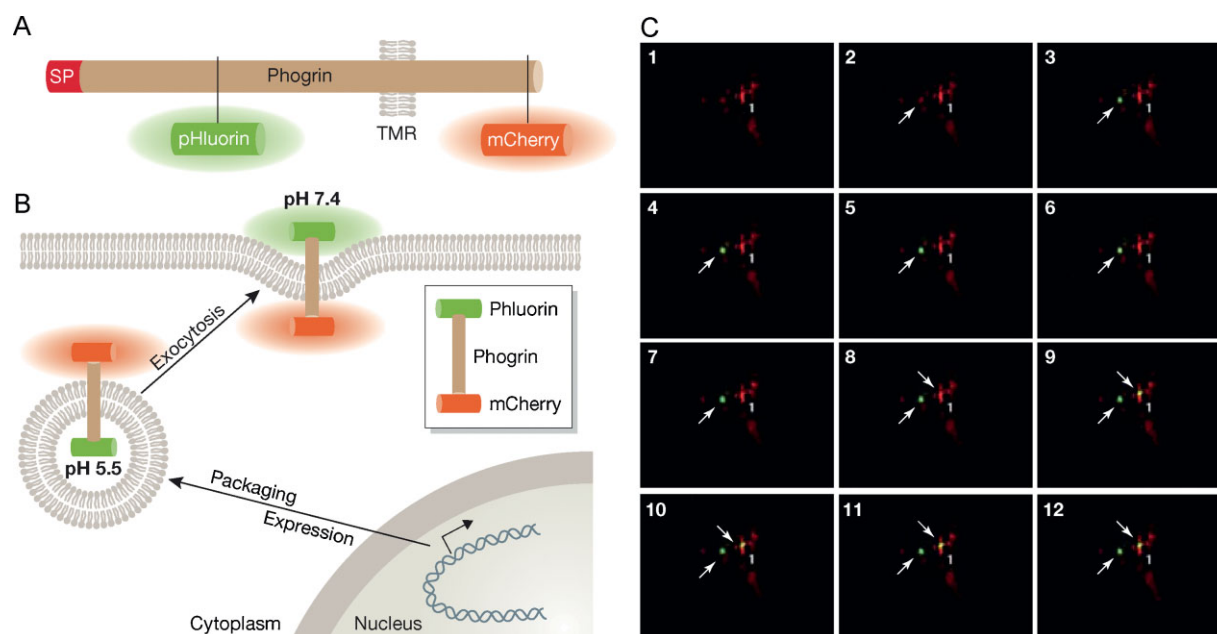
Figure 4. An optical sensor for visualizing insulin granule exocytosis.

A. The sensor is based on a chimeric fusion protein that consists of a secretory granule resident protein, phogrin and two fluorescent proteins: a highly pH-sensitive pHluorin inside the secretory granules and a red mCherry.

B. Schematic showing the design strategy of the optical sensor. pHluorin is inside the acidic lumen and remains non-fluorescent at resting state. Upon exocytosis, pHluorin faces the extracellular fluid at neutral pH, and becomes highly fluorescent, while mCherry remains in the cytosol during the process, and serves as a label for granule tracking and a standard for ratiometric quantification (adapted from Lu et al, 2009).

C. A time-lapse showing detected exocytosis events in insulin-secreting cells. Arrows indicate exocytosed insulin granules. SP, signal peptide; TMR, transmembrane region. The images are unpublished observations by Gustavsson.

clear (Kahn et al, 2009). It is thus important to quantify β-cell mass *in vivo* and to correlate it with glucose homeostasis in the course of diabetes development. Furthermore, determining β-cell mass and function *in vivo* is essential to assess tissue- and cell-based therapies for diabetes.

From the drug development angle, an animal model that allows detection of β-cell mass *in vivo* will be extremely useful to evaluate the potential of drug candidates in preserving β-cell function and number, but imaging the pancreas in small animals is challenging as it is a thin layer of tissue of irregular shape between other large organs. Imaging pancreatic islets to evaluate the β-cell mass is even more difficult because the islets occupy only 1–2% of the total pancreas volume. In addition, motion artefacts due to respiration and cardiac pulsation may deteriorate the quality of high resolution imaging needed for resolving the pancreas. Due to the lack of difference in proton density and MRI relaxation times between β-cells and surrounding pancreatic tissues, β-cells cannot be differentiated based on these intrinsic contrasts in MRI. Although contrast agents can be designed to target specific receptors on cells, the limited number of receptors on β-cell surface requires high sensitivity, affinity and specificity of the contrast agent (for review of past efforts on developing β-cell imaging probes, see Schneider, 2008). As this likely represents the best translatable approach for non-invasive imaging of human β-cell mass, ongoing efforts are aimed at identifying novel β-cell specific

biomarkers (Flamez et al, 2010; Ueberberg et al, 2010). So far, limited success has been achieved in imaging β-cell mass in rodents by MRI of transplanted islets or β-cells labelled with iron oxide nanoparticles or gadolinium (Gd) (Evgenov et al, 2006; Zheng et al, 2005), by bioluminescent imaging of genetically introduced luciferase gene in β-cells (Park & Bell, 2009), by Mn^{2+}-enhanced MRI (Antkowiak et al, 2009) and by positron emission tomography (PET) imaging of dihydrotetrabenazine (DTBZ) bound Type 2 vesicular monoamine transporters (VMAT2) (Souza et al, 2006). We propose here two approaches to generate pancreatic β-cell specific labels that may allow quantification of β-cell mass *in vivo*.

Small molecule probes

Commonly used antibody-based imaging techniques are limited to tissue/cell surface targets (not intracellular) and repeated treatment may induce adverse immune responses. Tagging the antibodies with suitable labels (*e.g.* small molecules, metal complexes or nanoparticles) is an added challenge. Genetic modification of specific protein targets with fluorescence proteins such as green fluorescent protein (GFP) provides target specific labelling platforms in live systems but this approach is not applicable to a clinical setting limiting their usage to cell culture or animal model studies. Instead, small molecule probes are ideal for clinical application as demonstrated in many currently used drug molecules. Drug-like
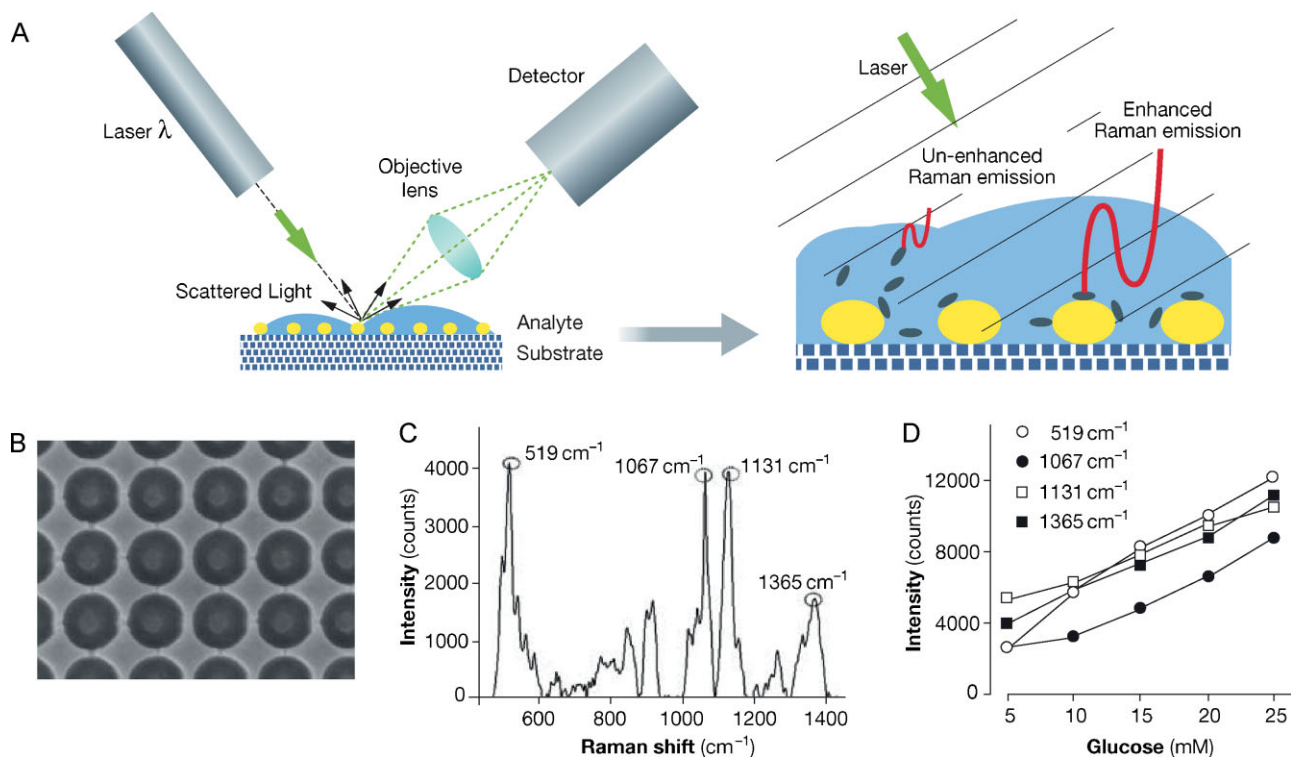
Figure 5. Basic concept and applications of surface-enhanced Raman spectroscopy.

A. Basic concept of SERS. Raman scattering occurs at very low intensities in solution phase when molecules (oval-shaped grains) are distant from the metallic nanoparticles (yellow spheres). When the molecule is close to the nanosurface, upon laser excitation, the intensity is enhanced by the interaction of the molecule with the surface electrons.

B. Scanning EM image of silver and gold bimetallic SERS substrate by deep UV lithography on silicon wafers designed for glucose sensing.

C. Raman spectrum of glucose. Glucose sensing using surface functionalized bimetallic SERS substrate shown in 5B in SERS mode. The peaks indicate different vibrational levels in the molecules. Note that the narrowness of the peaks allows structurally similar multiple analytes to be detected simultaneously.

D. Glucose quantification by SERS-based glucose sensing. Areas-under-curves of the vibrational bands of glucose Raman spectrum at 519, 1067, 1131 and 1365 cm^{-1} are plotted against glucose concentrations.

Table 1. Strategies for attaching an analyte molecule to the metal surface and applications

Technique	Principle	Current/potential applications	References
Polymer encapsulation	SERS reporter molecule on nanoparticle surface protected by thiol terminated polyethylene glycol	Non-invasive *in vivo* SERS imaging	Cho et al (2010); Qian et al (2008)
Silica encapsulation	SERS reporter molecule on nanoparticle surface protected by growing a shell of silica around the nanoparticle	Non-invasive *in vivo* SERS imaging	Keren et al (2008); Sha et al (2008); Zavaleta et al (2008, 2009)
Covalent anchor	Attaching the SERS reporter molecule covalently using thiol chemistry	Mammalian cell surface imaging	Hu et al (2007)
Self-assembled monolayer	Partition of an analyte into the monolayer on a SERS active substrate	*In vitro* and *in vivo* glucose sensing	Dinish et al (2009); Stuart et al (2006); Yonzon et al (2004)

BOX 3: How to target small molecule fluorescent probes

There are two general approaches to target small molecule fluorescent probes: one is analyte-oriented and the other diversity-oriented. The conventional analyte-oriented approach combines known analyte binding motifs to fluorescent molecules through a linker. Many fluorescence-based sensors have been developed through this approach, but each individual development requires a major effort in both designing and synthesizing the sensors and the sensor's application remains limited to the pre-selected specific analytes. To overcome this limitation and to accelerate novel sensor discovery, an alternative diversity oriented fluorescence library approach (DOFLA) was introduced recently (Lee et al, 2009b). In DOFLA, structurally diverse library compounds are generated by combinatorial chemistry and the library compounds are screened in high throughput manner either in purified analyte or against whole cell/tissue/organism. In addition to its high speed of novel probe discovery, this approach is advantageous over conventional method especially when the molecular target is not known, *i.e.* the whole cell can be used for screening, and the target can be identified later (system to target approach). DOFLA has been successfully used to generate probes against a broad range of targets including DNA (Lee et al, 2003), RNA (Li & Chang, 2006), β-amyloid (Li et al, 2004, 2007), GTP (Wang & Chang, 2006), heparin (Wang & Chang, 2008), chymotrypsin (Wang & Chang, 2008), human serum albumin (Ahn et al, 2008), glutathione (Ahn et al, 2007; Min et al, 2007) and myotube cell-state discrimination (Wagner et al, 2008).
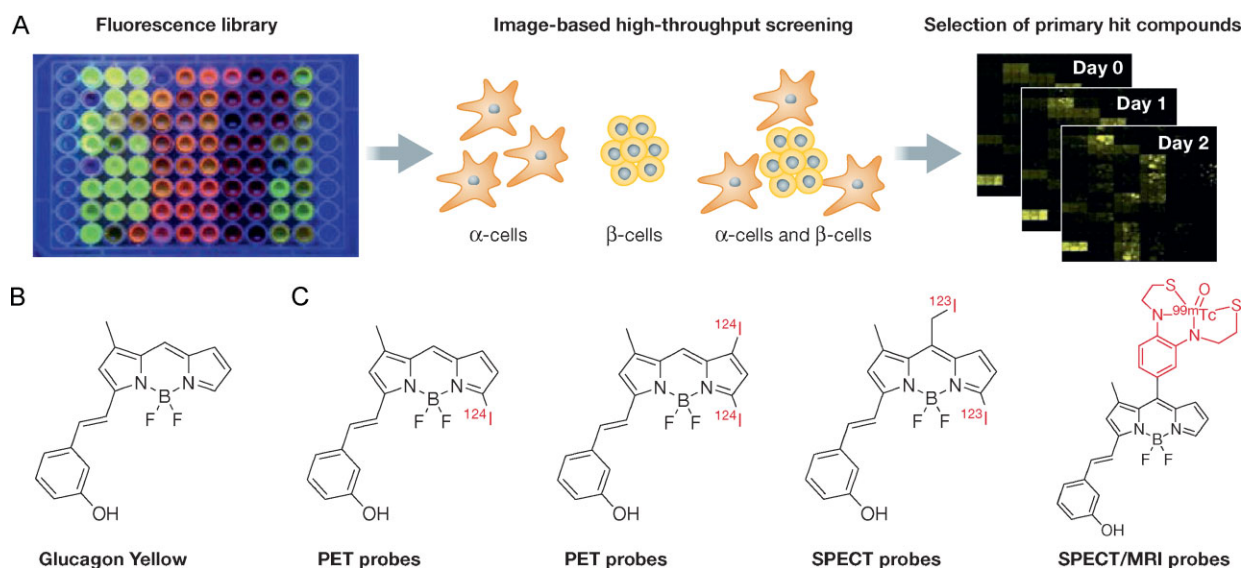

Figure 6. Schematic work flow of DOFLA in α- and β-cell screening and its application for *in vivo* imaging.
A. DOFLA preparation and high throughput screening in α- and β-cells to identify a probe specific for each of the cell types.
B. Structure of an α-cell selective probe Glucagon Yellow.
C. Examples of some potential modifications to convert Glucagon Yellow into PET or SPECT probes. The ^{99m}Tc ligand could also be replaced by a Gd chelate to form an MRI contrast agent.

imaging probes will also be easy-to-use universal research tools, which can be used in cell or animal studies, without additional genetic modifications. We note the revolutionary application of Fura dyes for calcium imaging; this powerful small molecule probe was the technical foundation for the booming of calcium signalling field during the last several decades (Grynkiewicz et al, 1985).

Despite their great potential, target specificity remains a challenge in developing small molecule probes. We discuss two approaches to target probes to particular molecules or cells in Box 3. Fluorescent molecules are the most popular small molecule probes due to their high sensitivity and exceptional ease of handling compared to their radioactive counterparts. However, the intrinsic limit of light penetration of the fluorescent probe precludes its applications in deep tissue imaging. They can, however, be modified by attaching an MRI-, PET- or SPECT (single photon emission computed tomography)-compatible functional group or single atomic radioisotope, which would render them suitable for deep tissue imaging in animal or clinical studies. The general work flow of diversity oriented fluorescence

library approach (DOFLA) (see Box 3) and strategies to convert a particular probe for MRI, PET and SPECT imaging are summarized in Fig 6. We have recently applied this approach to identify Glucagon Yellow as an α-cell-selective probe (Lee et al, 2009a). We believe that pancreatic β-cell specific probes can be identified by adopting the approaches described in Box 3, and that the identified fluorescent probe can be converted as in Fig 6 to allow quantification of β-cell mass *in vivo*.

Genetic approach

An alternative to the small molecule approach is by genetic introduction of complementary DNA (cDNAs) encoding proteins that bind to MRI-, PET- or SPECT-compatible probes, or that can accumulate iron and form MR-detectable iron particles. Although this cannot be adapted to clinical usage, applying it to animal models could generate useful pre-clinical models to evaluate therapeutic compounds for their ability to preserve β-cell mass. Several studies have demonstrated the use of iron-binding proteins such as ferritin and a bacterial protein MagA in *in vitro* and *in vivo* imaging (Cohen et al, 2005, 2007; Genove et al, 2005; Goldhawk et al, 2009; Zurkiya et al, 2008). One can envisage the use of transgenic mice expressing one of these proteins specifically in pancreatic β-cells for the detection and quantification of β-cell mass.

Functional assessment of pancreas *in vivo*

Pancreatic blood flow, blood volume and vascularization can provide valuable information on the pancreatic islet function and the re-establishment of β-cell function after transplantation. Dynamic contrast enhanced MRI with intravenous injection of Gd-based contrast agent has been used to estimate these haemodynamic parameters in humans (Coenegrachts et al, 2004; Yu et al, 2009). Since one passage of the contrast agent through circulation can be as short as 5 s in mice (Nyman et al, 2008) and 20 s in human, this makes it difficult to calculate blood flow from the very fast contrast agent kinetics. Instead, the time-to-peak and the area under curve of the contrast agent kinetics are commonly used as an estimate of blood volume and vascularization (Hathout et al, 2007; Medarova et al, 2007). We recently demonstrated that similar contrast agent enhanced MRI can be applied to study blood flow in mouse pancreas (Lee et al, 2009c). Another approach for quantifying blood flow is arterial spin labelling (Schraml et al, 2008), but this has its own share of challenges as well. A method based on gradient spin echo (GRASE) image acquisition can significantly reduce the susceptibility artefacts (unpublished observations) and could be applied in abdominal imaging. The present MR technologies cannot compete with the stunning time-resolved blood flow patterns of exposed mouse pancreas in 3D obtained by line-scanning confocal microscopy (Nyman et al, 2008). However, image registration and correlation of high resolution optical image data with MRI can provide a way for translating animal model observations to *in vivo* and to human studies.

Imaging glucose, its derivatives and the activation of β-cells *in vivo* is another important functional readout of the pancreas.

Glucose and glycogen can be detected by MRI using specific paramagnetic lanthanide complexes, which generate a chemical exchange saturation transfer (CEST) effect (Zhang et al, 2003). Glucose distribution in the liver has been mapped *ex vivo* in this manner (Ren et al, 2008). However, due to strong magnetic field heterogeneity and motion, it will prove to be difficult to apply this approach in *in vivo* studies. Using manganese ion (Mn^{2+}) as a calcium analogue allows the measurement of calcium influx into pancreatic β-cells after glucose stimulation (for review, please see Koretsky & Silva, 2004). Indeed, Mn^{2+}-enhanced MRI has been used to observe β-cell activity in isolated β-cells (Gimi et al, 2006) and in mouse pancreas *in vivo* (Antkowiak et al, 2009). Although the toxicity of Mn^{2+} may limit its application in humans, this non-invasive technique complements the restriction of optical fluorescent imaging.

Although MRI is sensitive to different physical and physiological parameters *in vivo*, it detects the ensemble of all the parameters and cannot differentiate individual components. This limits our ability to image multiple cell/islet populations and/or biological processes in parallel to understand their interactions and dynamics. One strategy to overcome this limitation is by using frequency-shifting contrast agents to change the resonance frequency of the water instead of changing the T_1 or T_2 relaxation times (Zabow et al, 2008). This allows images to be generated at different frequencies like quantum dots in optical imaging. Alternatively, one can combine the use of conventional relaxation agents (*e.g.* iron oxide nanoparticles or Mn^{2+}) and a CEST contrast agent (Gilad et al, 2009). A potential application is to track transplanted β-cells with iron oxide (or a frequency-shifting agent) and to monitor their function using Mn^{2+}- or Zn^{2+}-sensitive agents and/or CEST effect.

New technologies in imaging metabolic diseases

MRS using carbon (^{13}C) is ideally suited to the study of metabolism due to the extensive range of compounds that can be detected and the ability to attribute signals to the different carbon atoms within individual molecules. ^{13}C studies of metabolism in cells and *in vivo* have been conducted since the early 1980s, pioneered by Robert Shulman. Bailey et al carried out the first experiments on isolated perfused rat hearts using ^{13}C-enriched sodium acetate (Bailey et al, 1981). A wealth of work has since followed on cardiac metabolism, despite limitations of the method caused by both the low natural abundance of the MRS-visible isotope of carbon (^{13}C) and the low level of magnetic polarization normally achievable. The low natural abundance of ^{13}C has required most work to be conducted using ^{13}C-enriched molecules and even then long scan times are required, resulting in the study of metabolic steady-state conditions.

Recently, a new technique—DNP-MR—has produced a practical method to enhance magnetic polarization levels by more than 10,000-fold (Ardenkjaer-Larsen et al, 2003; Golman et al, 2003) (Fig 7). The technique combines the solid-state methods of dynamic nuclear polarization (DNP) (Bailey et al, 1981) with a rapid dissolution procedure to produce stable injectable solutions (*in vivo* stability of approximately 60 s)
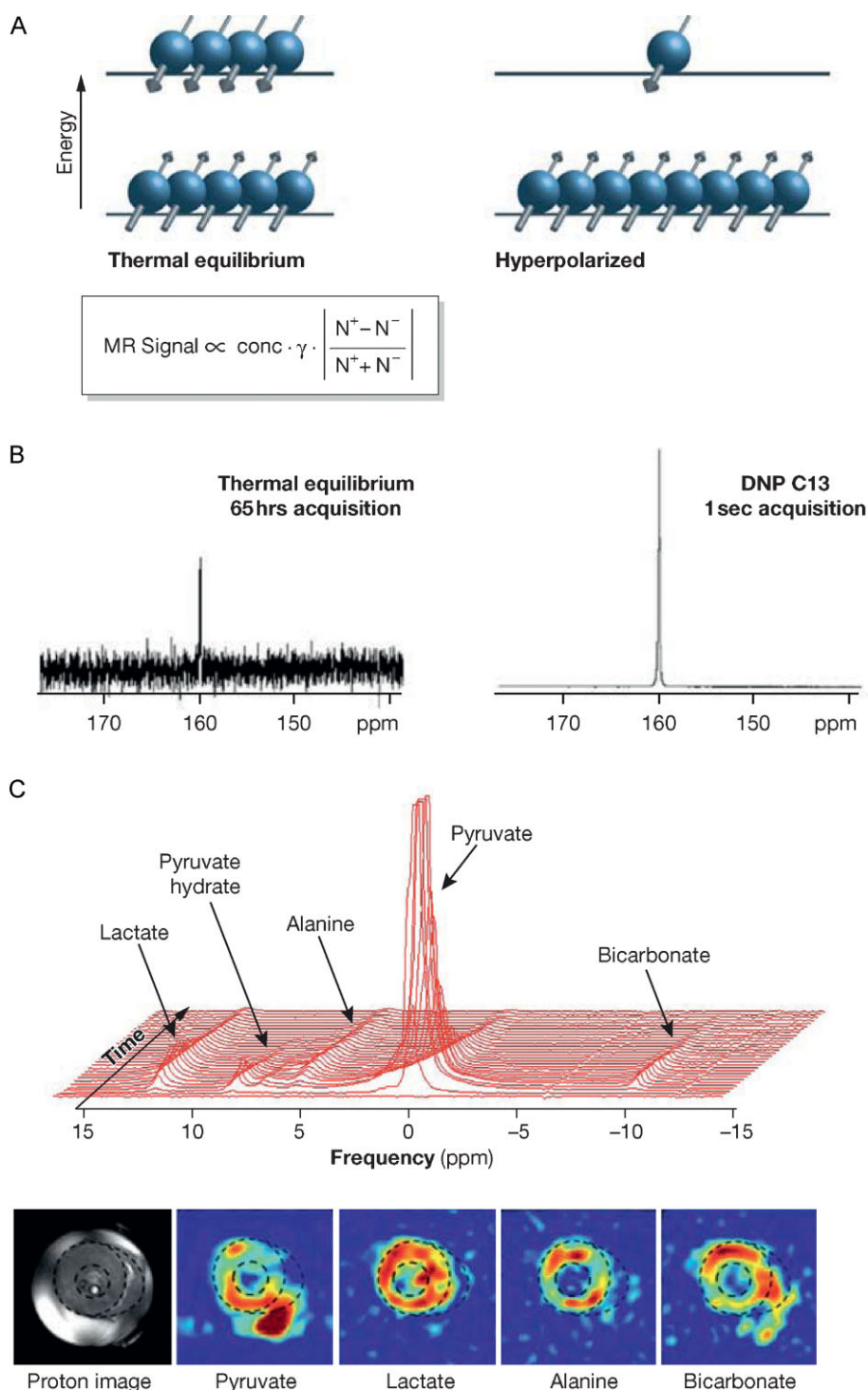
Figure 7. Hyperpolarized ^{13}C and an example of its applications in metabolic research.

A. The NMR signal is proportional to the difference between two populations of nuclei in distinct energy levels. Hyperpolarization of the ^{13}C nuclei produces a large difference as compared to the thermal equilibrium state thus increasing the NMR signal. N^+/N^-: number of nuclei in high/low energy state.

B. The thermal equilibrium ^{13}C spectrum of urea at 9.4 T averaged for 65 h is depicted on the left while the analysis of the same sample, hyperpolarized by the DNP-MR method and acquired in 1 s is presented on the right (adapted from Ardenkjaer-Larsen et al, 2003).

C. Time course of spectra acquired every second over a 60 s period after injection of hyperpolarized [1-^{13}C]pyruvate from the heart of a male Wistar rat (adapted from Tyler et al, 2008). As the pyruvate signal decays, one can observe the generation of lactate, alanine and bicarbonate. Chemical shift imaging of these metabolites from a perfused rat heart depicts the biodistribution. The proton image is given for anatomical reference. The images are unpublished observations by Lee.

Table 2. Summary of the technologies and approaches discussed in the article and their applications to the field of metabolism and metabolic syndrome

Applications	Technologies	Reporter	Subjects	Relevant reference
Quantification and 3D mapping of body fat	MRI and 1D MRS	Intrinsic/protons	Animal models and human subjects	Liu et al (2010); Springer et al (2010)
Detection and estimation of lipid saturation levels	2D MRS	Intrinsic/protons	Animal models and human subjects	Velan et al (2008))
Insulin measurement	ELISA or RIA	Antibody/fluorescence or radioactive	*In vitro*	Gustavsson et al (2008)
Visualization of insulin granules and their exocytosis	Fluorescent microscopy and intravital fluorescent microscopy	Fluorescent protein-fused secretory granule resident or cargo protein	*In vitro* and animal models	Lu et al (2009)
Detection and quantification of glucose	SERS	SERS-active substrates—Raman spectroscopy	*In vitro*, animal models and human subjects	Dinish et al (2009); Yonzon et al. (2004); Stuart et al. (2006)
β-Cell detection and β-cell mass determination	MRI	Iron oxide nanoparticles or gadolinium conjugates	*In vitro* and animal models	Evgenov et al (2006); Zheng et al (2005)
β-Cell detection and β-cell mass determination	MRI	Transgene encoding MRI-compatible probes (*e.g.* Ferritin and MagA)	Animal models	To be demonstrated
β-Cell detection and β-cell mass determination	Bioluminescence	Luciferase specifically expressed in β-cells	Animal models	Park & Bell (2009)
β-Cell detection and β-cell mass determination	Mn^{2+}-enhanced MRI	Manganese chloride	*In vitro* and animal models	Antkowiak et al (2009); Gimi (2006)
β-cell detection and β-cell mass determination	PET	DTBZ-bound VMAT2/positron emitting isotopes	Animal models	Souza et al (2006)
β-Cell detection and β-cell mass determination	MRI, PET, SPECT	DOFLA-based small molecule probes subsequently conjugated with imaging contrast agents	Animal models and human subjects	To be demonstrated
Detection and quantification of α-cells	MRI, PET, SPECT	Glucagon Yellow and other DOFLA-based small molecule probes subsequently conjugated with imaging contrast agents	Animal models and human subjects	Lee et al (2009a)
Assessment of pancreatic blood flow	Arterial spin labelling	Magnetically labelled blood–water	Animal models	Schraml et al (2008)
Assessment of pancreatic blood flow	GRASE	Proton diffusion measurements	Animal models	Unpublished
Assessment of pancreatic blood flow	Line-scanning confocal microscopy	Measurement of fluorescent probes	Animal models	Nyman et al (2008)
Tissue glucose distribution	CEST	Changes in proton density	Animal models	Ren et al (2008)
Detection of specific metabolite	MRS	^{13}C	*Ex vivo*	Bailey et al (1981)
Measurement of metabolic fluxes	DNP-MRS	Hyperpolarized ^{13}C	Animal models	Schroeder et al (2008, 2009)

Bridge the gap

The Gap

Metabolic syndrome, a pandemic problem in most of the developed countries and many developing nations, poses a significant burden to the health care of the affected countries. Despite intense efforts from both basic and clinical scientists, many fundamental questions regarding its aetiology and development remain unanswered. The fine details of *in vivo* insulin secretion regulation remain elusive. The threshold of β-cell mass needed to keep glucose level in check is not known. In addition, biomarkers that reflect *in vivo* β-cell mass or pancreatic activity are also needed as endpoints in clinical trials or for early drug development assays. Although many technologies are available to address these issues *in vitro* or *ex vivo*, what is urgently needed is clinical applicable technologies and proper animal models that can be used to understand the disease and test potential therapeutic candidates.

The Bridge

We believe imaging represents the most suitable technology in addressing these questions, with a track record of successful pre-clinical applications and clinical adaptation. Answering the questions above requires the development of suitable imaging tools and this Bridge the Gap article proposes a series of approaches that could be used to tackle these and other relevant matters in the field of metabolic diseases.

(Golman et al, 2006a; Malloy et al, 1987). DNP-MR allows visualization of ^{13}C-labelled metabolites *in vivo* and, more importantly, their enzymatic transformation into other species (Schroeder et al, 2008; Tyler et al, 2008).

Initial trials of the DNP-MR method focussed on the study of hyperpolarized [1-^{13}C]pyruvate (Golman et al, 2006b) and indicate that its rapid conversion to [1-^{13}C]lactate, [1-^{13}C]alanine and bicarbonate (H^{13}CO$_3^-$) should provide a sensitive test for cardiac metabolism. In the heart, the metabolism of pyruvate and the activity of mitochondrial pyruvate dehydrogenase (PDH) play key roles in oxidative metabolism (Chen et al, 2007; Schroeder et al, 2009). The development of metabolic imaging with hyperpolarized MR (Ardenkjaer-Larsen et al, 2003; Golman et al, 2006a) enabled unprecedented visualization of the biochemical mechanisms of normal and abnormal metabolism (Chen et al, 2007; Day et al, 2007; Golman et al, 2006b; Merritt et al, 2007), such as measuring PDH flux *in vivo*. *In vivo*, the hyperpolarized tracer [1-^{13}C]pyruvate rapidly generates the visible metabolic products [1-^{13}C]lactate, [1-^{13}C]alanine and bicarbonate (H^{13}CO$_3^-$), which exist in equilibrium with carbon dioxide (^{13}CO$_2$). Because it is the PDH-mediated decarboxylation of pyruvate into acetyl-CoA that produces ^{13}CO$_2$, monitoring the production of hyperpolarized H^{13}CO$_3^-$ should enable a direct, non-invasive measurement of flux through the PDH enzyme complex (Chen et al, 2007), which is highly dependent on PDH activity *in vivo*.

The Krebs cycle is fundamental to cardiac energy production, and is often implicated in energetic imbalances characteristic of heart disease. To date, Krebs cycle flux has been measured using ^{13}C-MR spectroscopy with isotopomer analysis; however, this approach is limited to the study of steady-state metabolism only and has limited *in vivo* applications. Hyperpolarized [2-^{13}C]pyruvate was demonstrated in a recent study to serve as a tracer to monitor Krebs cycle metabolism in the isolated perfused heart directly (Schroeder et al, 2009). Hyperpolarized [2-^{13}C]pyruvate was infused into healthy hearts, and the metabolic products with sufficient MR signal for detection at high temporal resolution were identified. The time courses of the formation of each of these metabolites gave kinetic information describing the relationships among cytosolic metabolism of [2-^{13}C]pyruvate, PDH-mediated oxidation of [2-^{13}C]pyruvate and its subsequent incorporation into the Krebs cycle. In addition, hyperpolarized [2-^{13}C]pyruvate was infused at the moment of reperfusion into globally ischaemic hearts, to identify differences in [2-^{13}C]pyruvate metabolism in the reperfused myocardium. This study demonstrated that Krebs cycle metabolism can be directly and instantaneously monitored by using hyperpolarized [2-^{13}C]pyruvate as a metabolic tracer, and that new information can be obtained about the coordination of glycolysis, pyruvate oxidation and Krebs cycle flux in the normal and post-ischaemic myocardium (Schroeder et al, 2009). Hence, hyperpolarized ^{13}C enables non-invasive, *in vivo* and real time assessment of metabolic processes, with the possibility of quantification, *e.g.* enzyme-mediated flux of metabolite intermediates (PDH, LDH (L-lactate dehydrogenase), CA). When coupled with metabolic imaging, it is possible to study the spatial distribution of metabolites and to measure *in vivo* pH at multiple time points (*e.g.* see Fig 7C). The technique may be applied to study the impact of carbohydrate metabolism on disease progression, and to evaluate the efficacy of therapeutic interventions longitudinally, *e.g.* to monitor glucose metabolism at different stages of diabetes development. Since α-cells, but not β-cells possess high level of surface transporters for pyruvate (monocarboxylase transporters) (Ishihara et al, 2003), a potential application of hyperpolarized imaging of pyruvate is to study the physiological and pathological changes specifically in pancreatic α-cells.

Although technical details are still being worked out, future applications of the technique in lipid metabolism will be highly significant in understanding changes in lipogenesis during development of obesity and other metabolic diseases.

Concluding remarks

Despite intense efforts from both basic and clinical scientists, many fundamental questions regarding the aetiology and development of the metabolic syndrome remain unanswered. We believe imaging represents the most suitable technology in addressing such questions, with a track record of successful pre-clinical applications and clinical adaptation. We discussed many imaging possibilities and approaches in this article and summarized them in Table 2. While some are currently in use, many others are still in early phase of development or of translation to clinical application. The diversity and the complexity of these approaches highlight the need for close collaborations among biologists, clinicians, chemists, physicists and engineers to develop suitable imaging tools that allow visualization of metabolic processes *in vivo*.

Acknowledgements

References

Ahn YH, Lee JS, Chang YT (2007) Combinatorial rosamine library and application to in vivo glutathione probe. J Am Chem Soc 129: 4510-4511

Ahn YH, Lee JS, Chang YT (2008) Selective human serum albumin sensor from the screening of a fluorescent rosamine library. J Comb Chem 10: 376-380

Antkowiak PF, Tersey SA, Carter JD, Vandsburger MH, Nadler JL, Epstein FH, Mirmira RG (2009) Noninvasive assessment of pancreatic beta-cell function in vivo with manganese-enhanced magnetic resonance imaging. Am J Physiol Endocrinol Metab 296: E573-E578

Ardenkjaer-Larsen JH, Fridlund B, Gram A, Hansson G, Hansson L, Lerche MH, Servin R, Thaning M, Golman K (2003) Increase in signal-to-noise ratio of >10,000 times in liquid-state NMR. Proc Natl Acad Sci USA 100: 10158-10163

Bailey IA, Gadian DG, Matthews PM, Radda GK, Seeley PJ (1981) Studies of metabolism in the isolated, perfused rat heart using 13C NMR. FEBS Lett 123: 315-318

Boesch C (2007) Musculoskeletal spectroscopy. J Magn Reson Imaging 25: 321-338

Boesch C, Slotboom J, Hoppeler H, Kreis R (1997) In vivo determination of intra-myocellular lipids in human muscle by means of localized 1H-MR-spectroscopy. Magn Reson Med 37: 484-493

Chen AP, Albers MJ, Cunningham CH, Kohler SJ, Yen YF, Hurd RE, Tropp J, Bok R, Pauly JM, Nelson SJ, et al (2007) Hyperpolarized C-13 spectroscopic imaging of the TRAMP mouse at 3T-initial experience. Magn Reson Med 58: 1099-1106

Cho SJ, Ahn YH, Maiti KK, Dinish US, Fu CY, Thoniyot P, Olivo M, Chang YT (2010) Combinatorial synthesis of a triphenylmethine library and their application in the development of surface enhanced Raman scattering (SERS) probes. Chem Commun (Cambridge, UK) 46: 722-724

Coenegrachts K, Van Steenbergen W, De Keyzer F, Vanbeckevoort D, Bielen D, Chen F, Dockx S, Maes F, Bosmans H (2004) Dynamic contrast-enhanced MRI of the pancreas: initial results in healthy volunteers and patients with chronic pancreatitis. J Magn Reson Imaging 20: 990-997

Cohen B, Dafni H, Meir G, Harmelin A, Neeman M (2005) Ferritin as an endogenous MRI reporter for noninvasive imaging of gene expression in C6 glioma tumors. Neoplasia 7: 109-117

Cohen B, Ziv K, Plaks V, Israely T, Kalchenko V, Harmelin A, Benjamin LE, Neeman M (2007) MRI detection of transcriptional regulation of gene expression in transgenic mice. Nat Med 13: 498-503

Day SE, Kettunen MI, Gallagher FA, Hu DE, Lerche M, Wolber J, Golman K, Ardenkjaer-Larsen JH, Brindle KM (2007) Detecting tumor response to treatment using hyperpolarized 13C magnetic resonance imaging and spectroscopy. Nat Med 13: 1382-1387

Dinish US, Chit YF, Agarwal A, Thoniyot P, Olivo M (2009) Glucose sensing using 3D array of reproducible surface enhanced Raman scattering substrates. Proc SPIE 7397: 73970C

Evgenov NV, Medarova Z, Dai G, Bonner-Weir S, Moore A (2006) In vivo imaging of islet transplantation. Nat Med 12: 144-148

Faulds K, Barbagallo RP, Keer JT, Smith WE, Graham D, (2004) SERRS as a more sensitive technique for the detection of labelled oligonucleotides compared to fluorescence. Analyst 129: 567-568

Flamez D, Roland I, Berton A, Kutlu B, Dufrane D, Beckers MC, De Waele E, Rooman I, Bouwens L, Clark A, et al (2010) A genomic-based approach identifies FXYD domain containing ion transport regulator 2 (FXYD2)gammaa as a pancreatic beta cell-specific biomarker. Diabetologia

Genove G, DeMarco U, Xu H, Goins WF, Ahrens ET (2005) A new transgene reporter for in vivo magnetic resonance imaging. Nat Med 11: 450-454

Gilad AA, van Laarhoven HW, McMahon MT, Walczak P, Heerschap A, Neeman M, van Zijl PC, Bulte JW (2009) Feasibility of concurrent dual contrast enhancement using CEST contrast agents and superparamagnetic iron oxide particles. Magn Reson Med 61: 970-974

Gimi B (2006) Magnetic resonance microscopy: concepts, challenges, and state-of-the-art. Methods Mol Med 124: 59-84

Gimi B, Leoni L, Oberholzer J, Braun M, Avila J, Wang Y, Desai T, Philipson LH, Magin RL, Roman BB (2006) Functional MR microimaging of pancreatic beta-cell activation. Cell Transplant 15: 195-203

Goldhawk DE, Lemaire C, McCreary CR, McGirr R, Dhanvantari S, Thompson RT, Figueredo R, Koropatnick J, Foster P, Prato FS (2009) Magnetic resonance imaging of cells overexpressing MagA, an endogenous contrast agent for live cell imaging. Mol Imaging 8: 129-139

Golman K, Ardenkjaer-Larsen JH, Petersson JS, Mansson S, Leunbach I (2003) Molecular imaging with endogenous substances. Proc Natl Acad Sci USA 100: 10435-10439

Golman K, in 't Zandt R, Thaning M (2006a) Real-time metabolic imaging. Proc Natl Acad Sci USA 103: 11270-11275

Golman K, Zandt RI, Lerche M, Pehrson R, Ardenkjaer-Larsen JH (2006b) Metabolic imaging by hyperpolarized 13C magnetic resonance imaging for in vivo tumor diagnosis. Cancer Res 66: 10855-10860

Grynkiewicz G, Poenie M, Tsien RY (1985) A new generation of Ca^{2+} indicators with greatly improved fluorescence properties. J Biol Chem 260: 3440-3450

Gustavsson N, Lao Y, Maximov A, Chuang JC, Kostromina E, Repa JJ, Li C, Radda GK, Sudhof TC, Han W (2008) Impaired insulin secretion and glucose intolerance in synaptotagmin-7 null mutant mice. Proc Natl Acad Sci USA 105: 3992-3997

Hathout E, Sowers L, Wang R, Tan A, Mace J, Peverini R, Chinnock R, Obenaus A (2007) In vivo magnetic resonance imaging of vascularization in islet transplantation. Transplant Int 20: 1059-1065

Hu Q, Tay LL, Noestheden M, Pezacki JP (2007) Mammalian cell surface imaging with nitrile-functionalized nanoprobes: biophysical characterization of aggregation and polarization anisotropy in SERS imaging. J Am Chem Soc 129: 14-15

Ishihara H, Maechler P, Gjinovci A, Herrera PL, Wollheim CB (2003) Islet beta-cell secretion determines glucagon release from neighbouring alpha-cells. Nat Cell Biol 5: 330-335

Kahn SE, Zraika S, Utzschneider KM, Hull RL (2009) The beta cell lesion in type 2 diabetes: there has to be a primary functional abnormality. Diabetologia 52: 1003-1012

Keren S, Zavaleta C, Cheng Z, de la Zerda A, Gheysens O, Gambhir SS (2008) Noninvasive molecular imaging of small living subjects using Raman spectroscopy. Proc Natl Acad Sci USA 105: 5844-5849

Kim JH, Kim JS, Choi H, Lee SM, Jun BH, Yu KN, Kuk E, Kim YK, Jeong DH, Cho MH, *et al* (2006) Nanoparticle probes with surface enhanced Raman spectroscopic tags for cellular cancer targeting. Anal Chem 78: 6967-6973

Korach-Andre M, Gao J, Gounarides JS, Deacon R, Islam A, Laurent D (2005) Relationship between visceral adiposity and intramyocellular lipid content in two rat models of insulin resistance. Am J Physiol Endocrinol Metab 288: E106-E116

Koretsky AP, Silva AC (2004) Manganese-enhanced magnetic resonance imaging (MEMRI). NMR Biomed 17: 527-531

Lee JW, Jung M, Rosania GR, Chang YT (2003) Development of novel cell-permeable DNA sensitive dyes using combinatorial synthesis and cell-based screening. Chem Commun (Cambridge, UK) 15: 1852-1853

Lee JS, Kang NY, Kim YK, Samanta A, Feng S, Kim HK, Vendrell M, Park JH, Chang YT (2009a) Synthesis of a BODIPY library and its application to the development of live cell glucagon imaging probe. J Am Chem Soc 131: 10077-10082

Lee JS, Kim YK, Vendrell M, Chang YT (2009b) Diversity-oriented fluorescence library approach for the discovery of sensors and probes. Mol Biosyst 5: 411-421

Lee P, Golay X, Radda GK (2009c) Dynamic Perfusion Study of Mouse Pancreas with an Intravascular Contrast Agent In *Proceedings of the International Society for Magnetic Resonance in Medicine*, Hawaii, USA, p 2057.

Li Q, Chang YT (2006) A protocol for preparing, characterizing and using three RNA-specific, live cell imaging probes: E36, E144 and F22. Nat Protoc 1: 2922-2932

Li Q, Lee JS, Ha C, Park CB, Yang G, Gan WB, Chang YT (2004) Solid-phase synthesis of styryl dyes and their application as amyloid sensors. Angew Chem Int Ed Engl 43: 6331-6335

Li Q, Min J, Ahn YH, Namm J, Kim EM, Lui R, Kim HY, Ji Y, Wu H, Wisniewski T, *et al* (2007) Styryl-based compounds as potential in vivo imaging agents for beta-amyloid plaques. Chembiochem 8: 1679-1687

Liu CY, Redheuil A, Ouwerkerk R, Lima JA, Bluemke DA (2010) Myocardial fat quantification in humans: evaluation by two-point water-fat imaging and localized proton spectroscopy. Magn Reson Med 63: 892-901

Lu J, Gustavsson N, Li Q, Radda GK, Sudhof TC, Han W (2009) Generation of transgenic mice for in vivo detection of insulin-containing granule exocytosis and quantification of insulin secretion. J Innov Opt Health Sci 2: 397-405

Malloy CR, Sherry AD, Jeffrey FM (1987) Carbon flux through citric acid cycle pathways in perfused heart by 13C NMR spectroscopy. FEBS Lett 212: 58-62

Medarova Z, Castillo G, Dai G, Bolotin E, Bogdanov A, Moore A (2007) Noninvasive magnetic resonance imaging of microvascular changes in type 1 diabetes. Diabetes 56: 2677-2682

Meex RC, Schrauwen-Hinderling VB, Moonen-Kornips E, Schaart G, Mensink M, Phielix E, van de Weijer T, Sels JP, Schrauwen P, Hesselink MK (2010) Restoration of muscle mitochondrial function and metabolic flexibility in type 2 diabetes by exercise training is paralleled by increased myocellular fat storage and improved insulin sensitivity. Diabetes 59: 572-579

Merritt ME, Harrison C, Storey C, Jeffrey FM, Sherry AD, Malloy CR (2007) Hyperpolarized 13C allows a direct measure of flux through a single enzyme-catalyzed step by NMR. Proc Natl Acad Sci USA 104: 19773-19777

Min J, Lee JW, Ahn YH, Chang YT (2007) Combinatorial dapoxyl dye library and its application to site selective probe for human serum albumin. J Comb Chem 9: 1079-1083

Muoio DM, Newgard CB (2006) Obesity-related derangements in metabolic regulation. Annu Rev Biochem 75: 367-401

Nyman LR, Wells KS, Head WS, McCaughey M, Ford E, Brissova M, Piston DW, Powers AC (2008) Real-time, multidimensional in vivo imaging used to investigate blood flow in mouse pancreatic islets. J Clin Invest 118: 3790-3797

Park SY, Bell GI (2009) Noninvasive monitoring of changes in pancreatic beta-cell mass by bioluminescent imaging in MIP-luc transgenic mice. Horm Metab Res 41: 1-4

Qian X, Peng XH, Ansari DO, Yin-Goen Q, Chen GZ, Shin DM, Yang L, Young AN, Wang MD, Nie S (2008) In vivo tumor targeting and spectroscopic detection with surface-enhanced Raman nanoparticle tags. Nat Biotechnol 26: 83-90

Reaven GM (1993) Role of insulin resistance in human disease (syndrome X): an expanded definition. Annu Rev Med 44: 121-131

Ren J, Trokowski R, Zhang S, Malloy CR, Sherry AD (2008) Imaging the tissue distribution of glucose in livers using a PARACEST sensor. Magn Reson Med 60: 1047-1055

Schneider S (2008) Efforts to develop methods for in vivo evaluation of the native beta-cell mass. Diabetes Obes Metab 10: 109-118

Schraml C, Schwenzer NF, Martirosian P, Claussen CD, Schick F (2008) Perfusion imaging of the pancreas using an arterial spin labeling technique. J Magn Reson Imaging 28: 1459-1465

Schroeder MA, Cochlin LE, Heather LC, Clarke K, Radda GK, Tyler DJ (2008) In vivo assessment of pyruvate dehydrogenase flux in the heart using hyperpolarized carbon-13 magnetic resonance. Proc Natl Acad Sci USA 105: 12051-12056

Schroeder MA, Atherton HJ, Ball DR, Cole MA, Heather LC, Griffin JL, Clarke K, Radda GK, Tyler DJ (2009) Real-time assessment of Krebs cycle metabolism using hyperpolarized 13C magnetic resonance spectroscopy. FASEB J 23: 2529-2538

Sha MY, Xu H, Natan MJ, Cromer R (2008) Surface-enhanced Raman scattering tags for rapid and homogeneous detection of circulating tumor cells in the presence of human whole blood. J Am Chem Soc 130: 17214-17215

Shi C, Zhang Y, Gu C, Chen B, Seballos L, Olson T, Zhang JZ (2009) Molecular fiber sensors based on surface enhanced Raman scattering (SERS). J Nanosci Nanotechnol 9: 2234-2246

Souza F, Simpson N, Raffo A, Saxena C, Maffei A, Hardy M, Kilbourn M, Goland R, Leibel R, Mann JJ, *et al* (2006) Longitudinal noninvasive PET-based beta cell mass estimates in a spontaneous diabetes rat model. J Clin Invest 116: 1506-1513

Springer F, Machann J, Claussen CD, Schick F, Schwenzer NF (2010) Liver fat content determined by magnetic resonance imaging and spectroscopy. World J Gastroenterol 16: 1560-1566

Stuart DA, Yuen JM, Shah N, Lyandres O, Yonzon CR, Glucksberg MR, Walsh JT, Van Duyne RP (2006) In vivo glucose measurement by surface-enhanced Raman spectroscopy. Anal Chem 78: 7211-7215

Tyler DJ, Schroeder MA, Cochlin LE, Clarke K, Radda GK (2008) Application of hyperpolarized magnetic resonance in the study of cardiac metabolism. Appl Magn Reson 34: 523-531

Ueberberg S, Ziegler D, Schechinger W, Dietrich JW, Akinturk S, Klein HH, Schneider S (2010) In vitro phage display in a rat beta cell line: a simple approach for the generation of a single-chain antibody targeting a novel beta cell-specific epitope. Diabetologia

Velan SS, Said N, Durst C, Frisbee S, Frisbee J, Raylman RR, Thomas MA, Rajendran VM, Spencer RG, Alway SE (2008) Distinct patterns of fat metabolism in skeletal muscle of normal-weight, overweight, and obese humans. Am J Physiol Regul Integr Comp Physiol 295: R1060-R1065

Vessby B, Gustafsson IB, Tengblad S, Boberg M, Andersson A (2002) Desaturation and elongation of fatty acids and insulin action. Ann N Y Acad Sci 967: 183-195

von Maltzahn G, Centrone A, Park JH, Ramanathan R, Sailor MJ, Hatton TA, Bhatia SN (2009) SERS-coded gold nanorods as a multifunctional platform for densely multiplexed near-infrared imaging and photothermal heating. Adv Mater 21: 3175-3180

Wagner BK, Carrinski HA, Ahn YH, Kim YK, Gilbert TJ, Fomina DA, Schreiber SL, Chang YT, Clemons PA (2008) Small-molecule fluorophores to detect cell-state switching in the context of high-throughput screening. J Am Chem Soc 130: 4208-4209

Wang S, Chang YT (2006) Combinatorial synthesis of benzimidazolium dyes and its diversity directed application toward GTP-selective fluorescent chemosensors. J Am Chem Soc 128: 10380-10381

Wang S, Chang YT (2008) Discovery of heparin chemosensors through diversity oriented fluorescence library approach. Chem Commun (Cambridge, UK) 10: 1173-1175

Xiao M, Nyagilo J, Arora V, Kulkarni P, Xu D, Sun X, Dave DP (2009) Gold nanotags for combined multi-colored Raman spectroscopy and X-ray computed tomography. Nanotechnology 21: 035101

Yonzon CR, Haynes CL, Zhang X, Walsh JT, Jr, Van Duyne RP (2004) A glucose biosensor based on surface-enhanced Raman scattering: improved partition layer, temporal stability, reversibility, and resistance to serum protein interference. Anal Chem 76: 78-85

Yu CW, Shih TT, Hsu CY, Lin LC, Wei SY, Lee CM, Lee YT (2009) Correlation between pancreatic microcirculation and type 2 diabetes in patients with coronary artery disease: dynamic contrast-enhanced MR imaging. Radiology 252: 704-711

Zabow G, Dodd S, Moreland J, Koretsky A (2008) Micro-engineered local field control for high-sensitivity multispectral MRI. Nature 453: 1058-1063

Zavaleta C, de la Zerda A, Liu Z, Keren S, Cheng Z, Schipper M, Chen X, Dai H, Gambhir SS (2008) Noninvasive Raman spectroscopy in living mice for evaluation of tumor targeting with carbon nanotubes. Nano Lett 8: 2800-2805

Zavaleta CL, Smith BR, Walton I, Doering W, Davis G, Shojaei B, Natan MJ, Gambhir SS (2009) Multiplexed imaging of surface enhanced Raman scattering nanotags in living mice using noninvasive Raman spectroscopy. Proc Natl Acad Sci USA 106: 13511-13516

Zhang S, Trokowski R, Sherry AD (2003) A paramagnetic CEST agent for imaging glucose by MRI. J Am Chem Soc 125: 15288-15289

Zhang Y, Shi C, Gu C, Seballos L, Zhang JZ (2007) Liquid core photonic crystal fiber sensor based on surface enhanced Raman scattering. Appl Phys Lett 193504: 193504

Zhang X, Yin H, Cooper JM, Haswell SJ (2008) Characterization of cellular chemical dynamics using combined microfluidic and Raman techniques. Anal Bioanal Chem 390: 833-840

Zheng Q, Dai H, Merritt ME, Malloy C, Pan CY, Li WH (2005) A new class of macrocyclic lanthanide complexes for cell labeling and magnetic resonance imaging applications. J Am Chem Soc 127: 16178-16188

Zurkiya O, Chan AW, Hu X (2008) MagA is sufficient for producing magnetic nanoparticles in mammalian cells, making it an MRI reporter. Magn Reson Med 59: 1225-1231